Journal of Applied Polymer Science

Grafting of Maleic Anhydride onto an Ethylene-Propylene-Diene Terpolymer and Concurrent Organoclay Nanocomposite Preparation in Solution and Melt

Matjaž Krajnc,[1] József Karger-Kocsis,[2] Urška Šebenik[1]

[1]Department of Chemical Technology, Faculty of Chemistry and Chemical Technology, University of Ljubljana, Aškerčeva cesta 5, SI-1001 Ljubljana, Slovenia

[2]Polymer Engineering, Faculty of Mechanical Engineering, Budapest University of Technology and Economics, H-1111 Budapest, Hungary

Correspondence to: U. Šebenik (E-mail: urska.sebenik@fkkt.uni-lj.si)

ABSTRACT: The possibility of simultaneous peroxide-initiated grafting of MAH (maleic anhydride) onto EPDM (ethylene-propylene-diene terpolymer) and EPDM/clay nanocomposite synthesis by the solution and melt process is investigated. Montmorillonite organoclay is used. Maleation efficiency is investigated by infrared spectroscopy. Clay exfoliation and the resulting nanocomposite properties are determined by X-ray diffraction and dynamic mechanical analysis, respectively. Simultaneous grafting and exfoliated nanocomposite synthesis can be carried out in solution and melt. The use of optimal amounts of initiator and MAH is very important. High peroxide initiator concentration causes extensive EPDM crosslinking and scission reactions. High concentration of MAH deteriorates clay exfoliation in melt because of reduced shearing due to MAH addition. The use of low MAH concentration is a straightforward solution if the extent of MAH grafting onto EPDM is not considerably impaired. To overcome this problem, a two step melt compounding process is suggested and tried out. © 2012 Wiley Periodicals, Inc. J. Appl. Polym. Sci. 000: 000–000, 2012

KEYWORDS: functionalization of polymers; nanocomposites; rubber; organomodified montmorillonite

Received 6 March 2012; accepted 14 April 2012; published online
DOI: 10.1002/app.37898

INTRODUCTION

Nanoreinforcement of rubbers has a long and solid background. By far, the most popular nanofillers for rubber properties modification are carbon black and silica. For many decades also clay has been used as a filler for rubber mixes to set a beneficial property/cost balance. Incorporation of unmodified clay in a large amount resulted, however, in microcomposites.[1]

The majority of clay minerals belong to the category of layered silicates. Their principal building elements are two-dimensional arrays of silicon-oxygen tetrahedral and two-dimensional arrays of aluminium- or magnesium-oxygen/hydroxyl octahedral units, which are superimposed in different fashions. Partial replacement of trivalent Al by divalent Mg in the octahedral sheet results in a high negative surface charge of the layer. This fact renders the space between the layer surfaces capable of accommodating cations, such as Na^+ or K^+. An individual clay layer has a thickness under 1 nm and extends laterally up to 1 μm.[2] The nanolayers are not easily dispersed in most polymers due to their preferred face-to-face stacking in agglomerated tactoids. Dispersion of the tactiods into discrete nanolayers is further hindered by the intrinsic incompatibility of hydrophilic layered silicate and hydrophobic polymers. The replacement of inorganic cations in the intergalleries of the native clay (in the space between the layer surfaces) by organic cations increases the intergallery spacing and can compatibilize the surface chemistry of the clay and hydrophobic polymer matrix.[2] A widely accepted term for such clays, which are now commercially available, is "organoclays."

The concept of rubber "nanoreinforcement" with "organoclays" became very popular only recently. The high interest in research and development of rubber/organoclay nanocomposites is mostly due to the unexpected property improvements when clays are dispersed in nanometer scale, viz. when intercalation or exfoliation[1–4] of clay layers in rubber matrix is achieved. Intercalated nanocomposites are obtained only when the rubber chains are intercalated into the intergallery spacing. On the other hand, when the silicate layers are further pulled apart and appear exfoliated in the rubber matrix, exfoliated nanocomposites are obtained. Exfoliated nanocomposites comprise

dispersions of nano-clay platelets throughout a rubber matrix. A complete dispersion of clay nanolayers in a rubber matrix maximizes the number of available reinforcing elements and due to the high surface area ($\sim$760 m^2/g)[2] of clay particles, materials with improved properties can be synthesized at much lower amounts of clay as compared with traditionally used fillers and/or native clays. Improved mechanical performance, barrier properties, thermal stability, fire resistance, and wear behavior have been observed.[1]

The special character of rubber, being a multicomponent system (rubber or blend of different rubbers, curing agents, coagents, processing aids, reinforcements, fillers), complicates the analysis of the parameters affecting the rubber/clay nanocomposite formation. This was likely the reason for the late development of rubber/clay nanocomposites compared to thermoplastic or thermoset clay nanocomposites.[1] However, as substantial property upgrade in thermoplastic/organoclay and thermoset/organoclay nanocomposites was proved, research has been initiated also on the rubber/organoclay nanocomposites. Several rubbers and different methods, such as solution mixing, latex compounding, and melt mixing, to prepare rubber/clay nanocomposites have been used. The development of rubber/clay nanocomposites has been the subject of several review papers and book chapters.[1,5–7]

Ethylene-propylene-diene rubber (EPDM) has a wide application field, thus also the preparation and properties of its nanocomposites containing organoclay have been studied.[8–22] As EPDM is a highly nonpolar polymer, its functionalization by grafting of unsaturated polar groups onto the polymer backbone using organic peroxides as free radical initiators before its organoclay nanocomposite preparation may be appropriate. It has been shown that EPDM modified with maleic anhydride (MAH) mixes well with certain organoclays to form nanocomposites.[23–26]

Despite the large number of studies on MAH grafting and the commercial success of MAH grafted polyolefins, the chemical mechanism involved in the functionalization process is not fully understood. It has been shown that the reaction pathways depend on the polyolefin molecular structure.[27,28] It has been shown unambiguously that the MAH graft structure consists of single saturated MAH units.[29] Grafting occurs on secondary and/or tertiary carbons depending on the polyolefin composition. When long methylene sequences are present, it occurs mainly on secondary carbons.[30] Maleation occurs only on secondary carbons in polyethylene and ethylene-rich ethylene-propylene copolymers (EPMs), on tertiary carbons in polypropylene and propylene-rich EPMs and on both secondary and tertiary carbons for EPMs with intermediate compositions.[28] The MAH graft content is low for copolymers with high propylene content, it increases as the propylene content decreases and reaches a plateau at propene levels below 50 wt %.[27] For EPDM maleation occurs also on the unsaturated C=C bond of a diene.

However, grafting of MAH onto the EPDM backbone may be achieved by reactive melt processing[31–34] or in solution.[35–37] In both solution and melt grafting, the concentrations of peroxide and MAH have a significant effect on the MAH grafting efficiency and EPDM crosslinking. The latter usually accompanies grafting. In the melt, the MAH grafting is affected by the limited MAH solubility in the rubber and its high volatility at high temperatures. On the other hand, it has been observed that process variables, such as mixing temperature and time, rotor speed and filling grade of the mixing chamber, show only a marginal effect on the competing grafting and crosslinking reactions.[34] Moreover, not only rubber crosslinking but also significant chain scission, which is also induced by peroxide initiator, may occur during the melt method.[31,33–34,38–41] For polyethylene the dominant side reaction is crosslinking whereas for polypropylene it is chain scission. Therefore, in the case of EPDM reactive melt processing both are important. Change in the interfacial properties due to MAH grafting is associated with side reactions, such as crosslinking and chain scission, which may alter the rheological and processing characteristics of the functionalized polymer.[33] On the other hand, for EPDM maleation in solution it has been shown[37] that by optimization of process parameters, such as amounts of peroxide and MAH, reaction temperature and time may yield products with high grafted MAH and no gel contents. It has also been reported that MAH can be used as a clay modifier (it works as an intercalation agent for pristine montmorillonite clay) and a crosslinking agent for the EPDM matrix (if grafted MAH radicals terminate by combination), as well as a compatibilizer for EPDM and clay.[42,43]

The aim of the present investigation was to check whether peroxide-initiated grafting of MAH onto EPDM and preparation of EPDM/clay nanocomposite could be performed simultaneously. The MAH grafting and nanocomposite preparation were performed by the solution and melt process, as the maleation of EPDM and EPDM/clay nanocomposite production may be carried out both in solution and melt.

EXPERIMENTAL

Materials

The EPDM used was Royalene® 580HT EPDM (Lion Copolymer, LLC, Baton Rouge, Lousiana) with ethylene/propylene weight ratio 53/47 and 2.7 wt % of ethylidene norbornene. A commercial MAH (99.5% purity, Navast, China) was used for grafting. For solution grafting dibenzoyl peroxide (BPO, Aldrich, 70 wt %) as peroxide initiator was selected. BPO was recrystallized from absolute ethanol. As solvents xylene (Merck, $\geq$99.8%, Germany) and acetone (Sigma-Aldrich, $\geq$99.5%, Germany) were used. Dicumyl peroxide (DCP, Aldrich, 98%, Japan) was used for melt grafting. An organophilic clay Cloisite 15A (Southern Clay Products, Gonzales, Texas), which is a natural montmorillonite modified with *N, N*'-dimethyl, dihydrogenated tallow quaternary ammonium salt, was used in this work. The cation exchange capacity and basal spacing of Cloisite 15A reported by the supplier are 125 meq/100 g of clay and 3.15 nm, respectively.

Grafting and Concurrent Nanocomposite Preparation in Solution

EPDM (10.0 g) and MAH (4.0 g) were dissolved in xylene (200 g) in a glass reactor with four necks, equipped with a reflux condenser, a mechanical stirrer, a digital thermometer, and a nitrogen gas inlet. Clay (1.0 g) was added to the solution. The solution was stirred at 85 rpm (revolutions per minute) and purged with nitrogen over night. On the next day, a xylene

Table I. Sample Labels and Formulations

Sample	Method	EPDM (phr)	MAH (phr)	Clay (phr)	BPO (phr)	DCP (phr)
sEPDM-*g*-MAH	Solution	100	40	0	0.25	–
	Solution	100	40	0	0.50	–
	Solution	100	40	0	0.75	–
sEPDM-*g*-MAH/clay	Solution	100	40	10	0.75	–
sEPDM/I/clay	Solution	100	0	10	0.75	–
sEPDM/clay	Solution	100	0	10	0	–
sEPDM/I	Solution	100	0	0	0.75	–
mEPDM/MAH	Melt	100	10	0	–	0
mEPDM-*g*-MAH	Melt	100	10	0	–	0.25
	Melt	100	10	0	–	0.50
	Melt	100	10	0	–	1.00
	Melt	100	5	0	–	1.00
mEPDM-*g*-MAH/clay	Melt; 1 step	100	5	10	–	1.00
	Melt; 1 step	100	5	5	–	1.00
	Melt; 1 step	100	2.5	5	–	1.00
	Melt; 2 step	100 (50+50)[a]	2.5 (2.5+0)[a]	5 (5+0)[a]	–	1.00 (0.5+0.5)[a]
	Melt; 2 step	100 (50+50)[a]	2.5 (2.5+0)[a]	5 (0+5)[a]	–	1.00 (0.5+0.5)[a]
mEPDM/I/clay	Melt; 1 step	100	0	10	–	1.00
	Melt; 1 step	100	0	5	–	1.00
mEPDM/I	Melt	100	0	0	–	1.00

[a]phr added in 1st plus phr added in 2nd step of mixing.

solution of BPO (0.75 g) was slowly added to the reaction mixture. The total amount of xylene in the reactor was 250 g. The reaction mixture was refluxed for 1 h at 115°C. The product was precipitated out of xylene by adding acetone to the reaction mixture cooled to 80°C. The precipitate was separated from liquid phase by filtration. The maleated product was washed several times with acetone and exposed to vacuum at 50°C to reach a constant weight. Also the unreacted MAH was removed, which was confirmed by differential scanning calorimetric (DSC) analysis, which indicated no melting peak of MAH.

Three different composite materials were synthesized. The sEPDM-*g*-MAH/clay composite was prepared using the method described above. The sEPDM/I/clay composite was prepared as sEPDM-*g*-MAH/clay but without using MAH, while the sEPDM/clay was prepared as sEPDM-*g*-MAH/clay but without using MAH and initiator. Letter I stands for initiator in sample label.

To check the grafting efficiency and gel content of the maleated EPDM, also samples without organoclay (sEPDM-*g*-MAH) were prepared. Different initiator amounts (0.25, 0.50, and 0.75 phr; part per hundred part rubber) were used. The labels and detailed compositions of all samples are shown in Table I. The sample labeled sEPDM/I was prepared without MAH.

Grafting and Concurrent Nanocomposite Preparation in Melt

EPDM, MAH, clay, and DCP were mixed in an oil heated CW50 mixing chamber of a Brabender Platicorder (Dusseldorf, Germany). The mixing temperature was set to 125°C. The total mixing time was 20 min and the rotor speed was set to 50 rpm. First, EPDM was added into the mixing chamber. MAH, clay, and DCP were added after 2, 4, and 6 min of mixing, respectively. Samples of different compositions were prepared (Table I), and are labeled as follows: mEPDM-*g*-MAH/clay-materials obtained by EPDM maleation with simultaneous EPDM/clay nanocomposite preparation; mEPDM/clay-EPDM/clay composite without using MAH and initiator; mEPDM/I/clay-EPDM/clay composite prepared in the presence of initiator, but without MAH; mEPDM-*g*-MAH-maleated EPDM; mEPDM/MAH-a blend of EPDM and MAH without initiator.

The nanocomposites were prepared in one and two step mixing procedures. For the two-step mixing two variants were used. They differed from each another only in the introduction of the organoclay, as shown in Table I. Previous to all analyses, all the products were exposed to vacuum (at 80°C) to remove unreacted MAH residuals.

Characterization

Gel content of the grafted rubber was determined by Soxhlet extraction in boiling xylene for 24 h. The solution was filtered and the insoluble fraction was dried in vacuum at 70°C for 48 h before weighing. The gel content was defined as the weight fraction of the insoluble part.

As the grafted EPDM had a high gel content, titrimetric analysis for determination of the grafted MAH content was not suitable. To check and compare the grafting efficiency Fourier Transform Infrared-Attenuated Total Reflectance (FTIR-ATR) spectra of MAH, EPDM, and EPDM-*g*-MAH samples were collected on Bruker IFS 66/S spectrometer (Karlsruhe, Germany) and compared. As an indication of grafting efficiency for EPDM-*g*-MAH

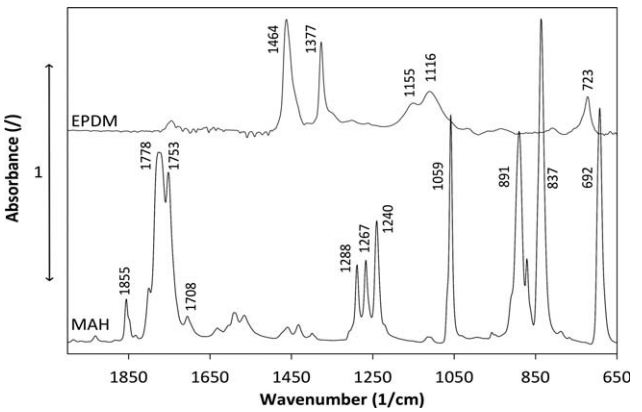

Figure 1. FTIR spectra in the 2000–650 cm^{-1} region for pure EPDM and pure MAH.

samples, the ratio between the area of peaks occurring between 1830 and 1660 cm^{-1} ($A_{1830–1660}$) and the area of the peak occurring between 1400 and 1320 cm^{-1} ($A_{1400–1320}$) were calculated. Furthermore, to determine the grafting efficiency quantitatively, a calibration curve showing dependence of $A_{1830–1660}/A_{1400–1320}$ ratio on MAH concentration was constructed. For this purpose, standard mixtures of EPDM with different MAH contents were prepared by mixing MAH and EPDM (without initiator) on a Brabender Plasticoder at 125°C. The total mixing time was 20 min, MAH was added after 2 min, and the rotor speed was 50 rpm. The amount of MAH in standard mixtures was determined titrimetrically. The titrimetric method is described elsewhere.[34]

The nanocomposite structure was characterized by means of X-ray diffraction (XRD). The XRD was measured with Cu Kα1 radiation generated at 45 kV and 40 mA using a PANalytical X'Pert PRO (PANalytical, Almelo, Netherlands). Approximately, 3 mm thick and 25 mm wide flat square samples were prepared and investigations carried out in the angle (2θ) range of 1.5–15° with a step of 0.034°.

Dynamic mechanical properties of materials were measured in shear mode on DMA861^e instrument (Mettler Toledo, Schwerzenbach, Switzerland). Samples were prepared in the disc shape (about 2 mm thick and with radius of about 12 mm). Linearity check was carried out and the measurements were performed within the linear viscoelastic regime. The dynamic mechanical properties were recorded at constant frequency of 1 Hz as a function of temperature (from −70 to 80°C) using a constant heating rate 2°C·min^{-1}.

To check the amount of clay built in a nanocomposite material, thermogravimetric analysis (TGA) tests for clay, EPDM, EPDM/clay, and EPDM-*g*-MAH/clay samples were performed on TGA/DSC1 instrument (Mettler Toledo, Schwerzenbach, Switzerland) using STAR 9.20 software. About 20 mg samples were placed in a 70 μL Al_2O_3 crucible. All the experiments were conducted in air atmosphere with a flow rate of 30 mL/min. A heating rate of 25°C·min^{-1} was used. Samples were heated to 700°C. For all measurements the baseline was subtracted. The amount of clay was calculated from the residual mass obtained at the end of TGA experiments.

RESULTS AND DISCUSSION

Figure 1 shows the FTIR spectra in the 2000–650 cm^{-1} region for pure EPDM and pure MAH. MAH gives rise to characteristic absorption bands at 1873–1820 cm^{-1} (unsaturated symmetric C═O stretching), 1820–1714 cm^{-1} (unsaturated asymmetric C═O stretching), and 717–661 cm^{-1} (C═C—H C—H bending). In regions 960–800 cm^{-1} and 1300–1000 cm^{-1} various absorption bands for C—O and C—C stretches occur. The peak at 1708 cm^{-1} indicates that MAH was partially hydrolyzed. In 2000–650 cm^{-1} region, characteristic absorption bands for EPDM were found at 1495–1409 cm^{-1} (CH_3 asymmetric C—H bending, CH_2 scissors C—H bending), 1400–1320 cm^{-1} (CH_3 symmetric C—H bending—umbrella mode), and 740–697 cm^{-1} (CH_2 rocking).

Figure 2 compares the FTIR spectrum for a standard mix prepared by EPDM mastication in the presence of MAH (without added initiator) with spectra for a sEPDM-*g*-MAH with 0.50 phr BPO and mEPDM-*g*-MAH with 1 phr DCP. Unreacted MAH has absorption bands in the same region as the grafted anhydride [Figure 2(a)].[34] The difference between unreacted and reacted MAH spectra is observable at 692 cm^{-1} [Figure 2(b)] where the characteristic absorption band for C—H bond

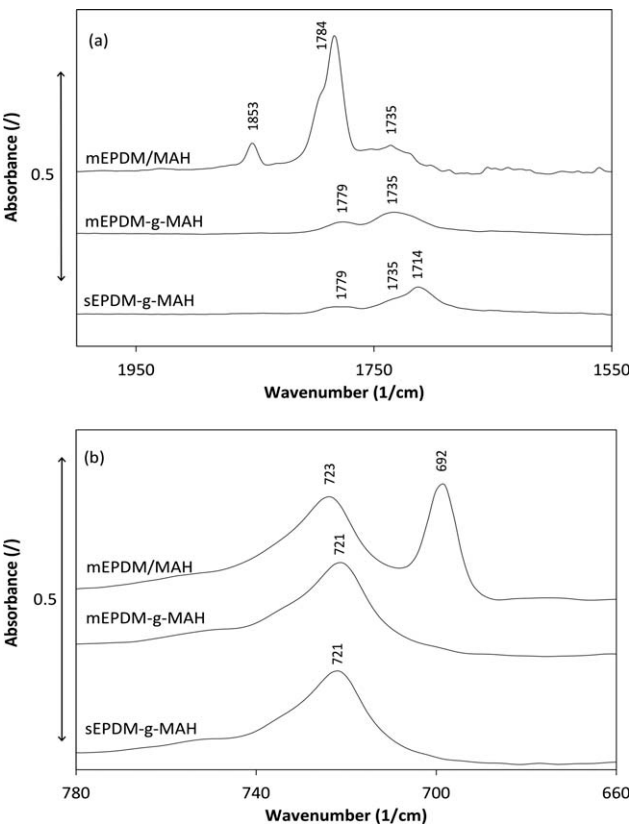

Figure 2. FTIR spectrum for a standard mix prepared by EPDM mastication in the presence of 10 phr MAH but without added initiator (mEPDM/MAH), and spectra for sEPDM-*g*-MAH (with 0.50 phr BPO) and for mEPDM-*g*-MAH (with 1 phr DCP) after vacuum exposure, both prepared with 10 phr MAH; (a) C═O group absorption band region, (b) CH_2 rocking and C═C—H C—H bending.

Table II. Gel Content Obtained by Soxhlet Extraction and Grafted MAH Content Evaluated on Calibration Curves

Sample	Initiator (phr)	MAH in formulation (phr)	Grafted MAH content (wt %)	Gel content (wt %)
sEPDM-g-MAH	0.25	40	0.72	64.0
	0.50	40	1.35	79.7
	0.75	40	0.95	78.1
sEPDM/I	0.75	0	-	0.3
mEPDM-g-MAH	0.25	10	0.60	44.0
	0.50	10	0.63	53.7
	1.00	10	1.14	63.9
	1.00	5	0.93	64.0
mEPDM/I	1.00	0	-	39.5

coupled to C=C of MAH appears. Spectra of sEPDM-*g*-MAH and mEPDM-*g*-MAH did not show the characteristic band at 692 cm^{-1}, as the unreacted MAH was successfully removed by vacuum exposure.

The results of grafted MAH content determination are shown in Table II together with those of gel determination. To obtain grafting efficiency for EPDM-*g*-MAH samples, the ratio between the area of MAH peaks occurring between 1830 and 1660 cm^{-1} ($A_{1830–1660}$) and the area of EPDM peak occurring between 1400 and 1320 cm^{-1} ($A_{1400–1320}$) was calculated. From the ratio values, the amount of grafted MAH was estimated using the calibration curve, which was constructed from data (the ratio values and corresponding MAH % content) for standard mixtures. Standard mixtures contained EPDM and unreacted MAH. Their MAH % was determined titrimetrically.

When the solution method was used, a maximum value of grafted MAH content was obtained at 0.50 phr of BPO. Something similar was observed by Xie et al.[37] They showed that with increasing initiator concentration the bond MAH content increases and reaches a maximum value. The increase corresponds to the increasing number of free radicals per EPDM molecule. Further increase of initiator concentration lowers the bond MAH content. This trend was ascribed[38] to combined effects deriving from: (i) MAH radicals have a low tendency to homopolymerize; (ii) partial saturation of reactive sites on EPDM chains; (iii) decreasing initiator efficiency due to recombination reactions among primary radicals, and (iv) increasing probability of crosslinking reaction of EPDM macroradicals. In our case, the amount of gel increased with increasing amount of BPO and reached a maximum value around 80 %, already when 0.50 phr of BPO was applied. Interestingly, sample sEPDM/I (no MAH in the formulation) contained only a minimal amount of gel, indicating that the presence of MAH contributed to gel formation. As MAH graft on to polymer backbones generally has only one MAH unit,[29,44] it is most likely that termination by combination was the reason for gel formation.

When the melt method was used, a maximum value of grafted MAH content was obtained at 1.0 phr of DCP and 10 phr of MAH. Wu et al.[33] have observed that the extent of grafting increases with MAH content at a fixed DCP level and with DCP content at a fixed MAH level. However, they also observed that the grafted MAH content reaches a plateau value. Once the plateau value is reached, a further increase in MAH or DCP content does not improve the grafting efficiency. A similar result was reported also by Grigoryeva et al.,[34] who used 2,5-dimethyl-2,5-di-(*t*-butylperoxy)hexane as initiator. They achieved maximum grafting of about 3 wt %, which is considerably higher than in this work. The lower grafted MAH content observed here may be ascribed also to the lower content of diene component in the EPDM used in our study (2.7 compared to 5 wt %[34]). The gel content increased with the DCP level (Table II), indicating termination by combination and/or that an important part of the free radicals generated from DCP was consumed in the EPDM crosslinking reaction. As the sample without MAH (mEPDM/I) contained gel (40 wt %), the EPDM crosslinking reaction was also confirmed. This was predictable, because the temperature and reactant concentrations were high enough. Moreover, the melt maleation processes with 1.00 phr of DCP ended by grinding of the crosslinked polymer into a powder, which has been observed also by Wu et al.[33] and Grigoryeva et al.,[34] who attributed this to extensive peroxide-initiated scission of partially crosslinked EPDM chains and the shear-assisted disruption of the crosslinked network structure. The chain scission should be considered responsible for the lower gel content in the samples obtained in the melt compared to those obtained by the solution method. Our intention was to prepare EPDM/clay and EPDM-*g*-MAH/clay composite materials with 1.00 phr of DCP and 5 phr of MAH, because in our case, at 1.00 phr of DCP, the grafted MAH content was the highest and comparable to that of the solution method. To our surprise, homogeneous blends, composed of elastomer, MAH, and clay, were obtained at the end of the melt mixing process. Apparently, the presence of clay hindered the crosslinking and chain scission reactions of the EPDM.

Nanocomposite Properties

First, the amount of clay incorporated into polymer matrixes (EPDM and EPDM-*g*-MAH) was checked by TGA analysis. The results are shown in Table III, where the determined clay content is given in wt %. If all the clay was efficiently incorporated into the rubber matrix, the clay contents should be 9.1 and 4.8 wt %, when 10 and 5 phr of clay was added in the recipes, respectively. The results in Table III indicate that both methods enabled rubber/clay composite preparation without significant loss of clay.

To answer the question if microcomposites or nanocomposites were obtained, XRD analysis was used. Determination of the morphology in a clay-containing nanocomposite requires the measurement of the interlayer spacing. Figure 3 shows XRD spectra of clay, EPDM, and sEPDM-*g*-MAH. The XRD pattern of organoclay had the highest peak at $2\theta = 2.8°$, which corresponded to an interlayer spacing of $d_{001} = 3.15$ nm. The peak detected at 2θ value around 7° was, according to data for pristine clay sold by the same producer ($d_{001} = 1.17$ nm), ascribed to unmodified clay fraction. The peak occurring like a shoulder of the highest peak between 4 and 5° indicates that Cloisite 15A

Table III. Clay Content in Composite Materials

Sample	Method	MAH (phr)	Clay in formulation (phr)	Initiator (phr)	Clay content (wt %)
sEPDM-*g*-MAH/clay	Solution	40	10	0.75	8.1
sEPDM/I/clay	Solution	0	10	0.75	8.6
sEPDM/clay	Solution	0	10	0	9.1
mEPDM-*g*-MAH/clay	Melt; 1 step	5	10	1.00	8.2
	Melt; 1 step	5	5	1.00	4.4
	Melt; 1 step	2.5	5	1.00	4.6
	Melt; 2 steps	2.5 (2.5+0)[a]	5 (5+0)[a]	1.00 (0.5+0.5)[a]	4.1
	Melt; 2 steps	2.5 (2.5+0)[a]	5 (0+5)[a]	1.00 (0.5+0.5)[a]	4.6
mEPDM/I/clay	Melt; 1 step	0	10	1.00	8.7
	Melt; 1 step	0	5	1.00	4.6

[a]phr added in 1st plus phr added in 2nd step of mixing.

contained also a fraction of modified clay with interlayer spacing lower than 3.15 nm. The shoulder cannot be a second order peak of peak $d_{001} = 3.15$ nm, because it would appear at 2θ value 5.6°. Note that no XRD peaks were observed for EPDM and sEPDM-*g*-MAH samples.

In Figure 4 spectra of rubber/clay composites obtained by the solution method are compared. The Cloisite 15A peak occurring at 2θ value 2.8° was not observed in the spectra of composites, indicating complete exfoliation of the clay fraction with an original interlayer spacing 3.15 nm. On the other hand, in XRD curves of composites without MAH (with and without DCP) two distinct peaks at 4.3 and 7.5° were observed. The positions of these peaks match the shoulder of the highest peak between 4 and 5°, and the peak of the pristine clay fraction, discernible also in the Cloisite 15A spectrum (cf. Figure 3). Accordingly, these fractions of clay did not exfoliate after clay incorporation into the highly nonpolar EPDM matrix. However, the intensity of these two peaks decreased significantly when MAH was added to the composite formulation (sEPDM-*g*-MAH/clay). The fact that the amount of dispersed clay was practically the same for sEPDM/clay and sEPDM-*g*-MAH/clay (Table III) may imply that most of the clay was successfully exfoliated in the latter compound.

Figure 5 shows XRD spectra of mEPDM/I/clay and mEPDM-*g*-MAH/clay composites. In the spectra three separate peaks can be observed. The Cloisite 15A peak occurring at 2θ value 2.8° (3.15 nm) shifted to 2.4° (3.68 nm), which indicates intercalation. Moreover, its intensity was lower than the intensity of the peak, which occurred just as a shoulder in Cloisite 15A spectrum, suggesting also some partial exfoliation. However, if spectra of samples with 5 phr of clay are compared, it may be concluded that 2.5 phr of MAH improved the exfoliation process, while 5 phr of MAH did not. This may be explained by torque lowering after MAH addition into the mixing chamber (MAH melting temperature is around 50°C), which was significant when 5 or more phr of MAH were used. To get intercalated/exfoliated nanocomposites, high shearing should be provided.[1] To check the validity of the given explanation, composites with 2.5 phr of MAH and 5 phr of clay were prepared using the two step method. The samples were prepared from sample mEPDM-*g*-MAH/clay with 5 phr of MAH and 10 phr of clay and sample mEPDM-*g*-MAH with 5 phr of MAH (without clay) by adding EPDM and EPDM plus clay during the second mixing step, respectively. To our delight, according to XRD results shown in Figure 6, we were able to conclude that after the second mixing step completely exfoliated nanocomposites

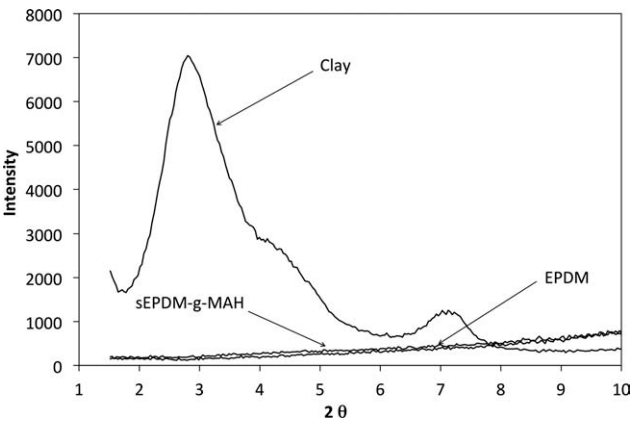

Figure 3. XRD spectra of clay (Cloisite 15A), EPDM, and sEPDM-*g*-MAH.

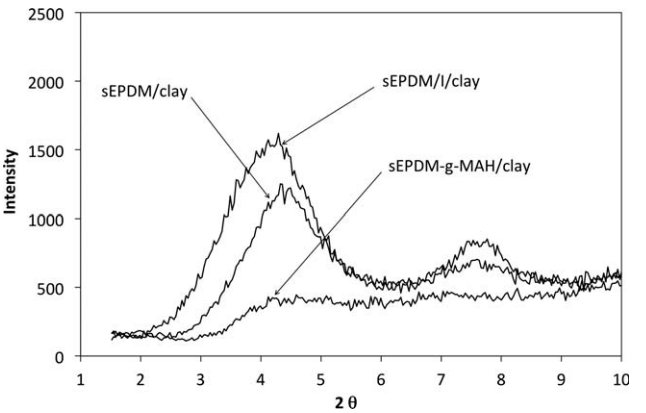

Figure 4. XRD spectra of clay (Cloisite 15A), EPDM, and sEPDM-*g*-MAH.

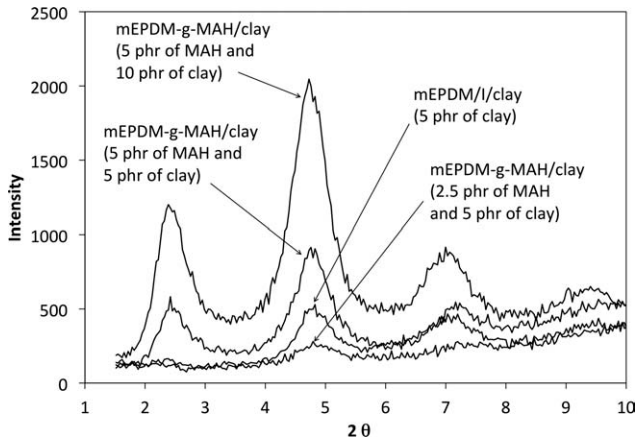

Figure 5. XRD spectra of mEPDM/I/clay (5 phr of clay) and mEPDM-*g*-MAH/clay composites (5 phr of MAH and 10 phr of clay; 5 phr of MAH and 5 phr of clay; 2.5 phr of MAH and 5 phr of clay).

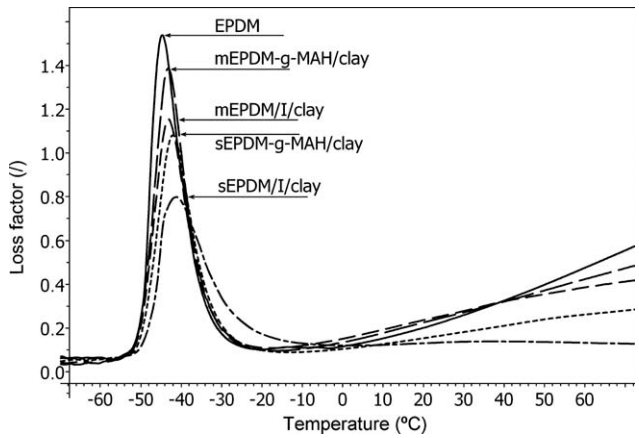

Figure 7. Loss factor curves versus temperature for samples with 10 phr of clay (sEPDM/I/clay, sEPDM-*g*-MAH/clay, mEPDM-*g*-MAH/clay and mEPDM/I/clay) and for neat EPDM.

were obtained, even when the clay was added only in the second step.

To monitor the reinforcing ability of layered silicates in the rubber matrix in the temperature range below and above the glass transition temperature (T_g) of the compound, dynamic mechanical analysis (DMA) appears to be an excellent tool. It has been shown that rubber nanocomposites with organoclay have a higher storage modulus and lower mechanical loss factor at polymer glass transition region if compared with neat rubber or rubber reinforced with unmodified clay.[1] In Figure 7 the loss factor versus temperature curves for samples sEPDM/I/clay, sEPDM-*g*-MAH/clay, mEPDM-*g*-MAH/clay, and mEPDM/I/clay, all containing 10 phr of clay, are shown and collated with that of the neat EPDM. Organoclay addition decreased the loss factor values (tanδ) at T_g and in the rubbery plateau region and increased T_g value to some extent (tanδ peak shifted to higher temperature). The composites prepared via the melt method had higher tanδ peak values than the composites prepared by the solution method. This substantiates that the solution method results in nanocomposites with higher reinforcing efficiency than the melt grafting/compounding route. The difference in the peak intensities of the related T_g peaks may be amplified by the extensive peroxide-initiated scission of the partially crosslinked EPDM chains and the shear-assisted disruption of the crosslinked network structure during reactive melt processing. Sample sEPDM/I/clay had the broadest glass transition region (a shoulder after tanδ peak was observed) which may be assigned to intercalated rubber chains possessing reduced mobility in the related intergallery (confined) space.[45]

Loss factor peak values of samples containing MAH were higher than those of samples without MAH (Figure 7). The effect of MAH charge during melt synthesis on composite loss behavior is shown more clearly in Figure 8, where tanδ curves for several mEPDM-*g*-MAH/clay samples and mEPDM/I/clay sample are depicted. Despite comparable tanδ peak heights one can notice that the higher the MAH content during melt mixing, the higher was the loss factor of the obtained product. Samples

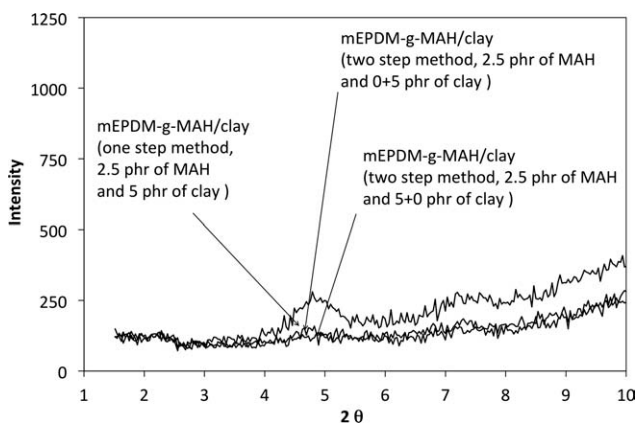

Figure 6. XRD spectra of mEPDM-*g*-MAH/clay composites with 2.5 phr of MAH and 5 phr of clay prepared by different methods; (5)-by one step method; (5+0)-by two step method where clay was added only in the first step; and (0+5)-by two step method where clay was added only in the second step.

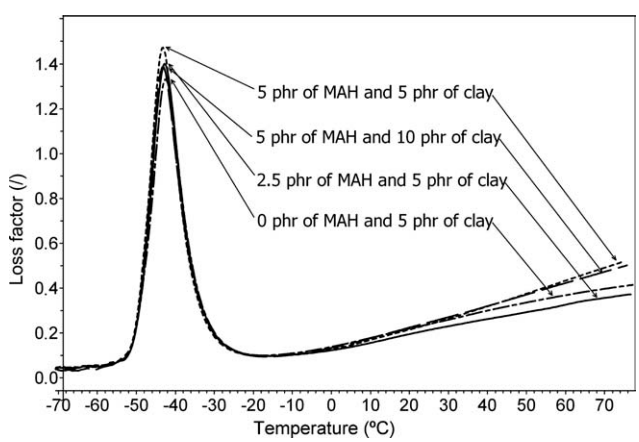

Figure 8. Loss factor curves versus temperature for mEPDM-*g*-MAH/clay samples with 5 phr of clay and 0.0, 2.5, and 5.0 phr of MAH. For comparison also the curve for sample with 10 phr of clay and 5.0 phr of MAH is shown.

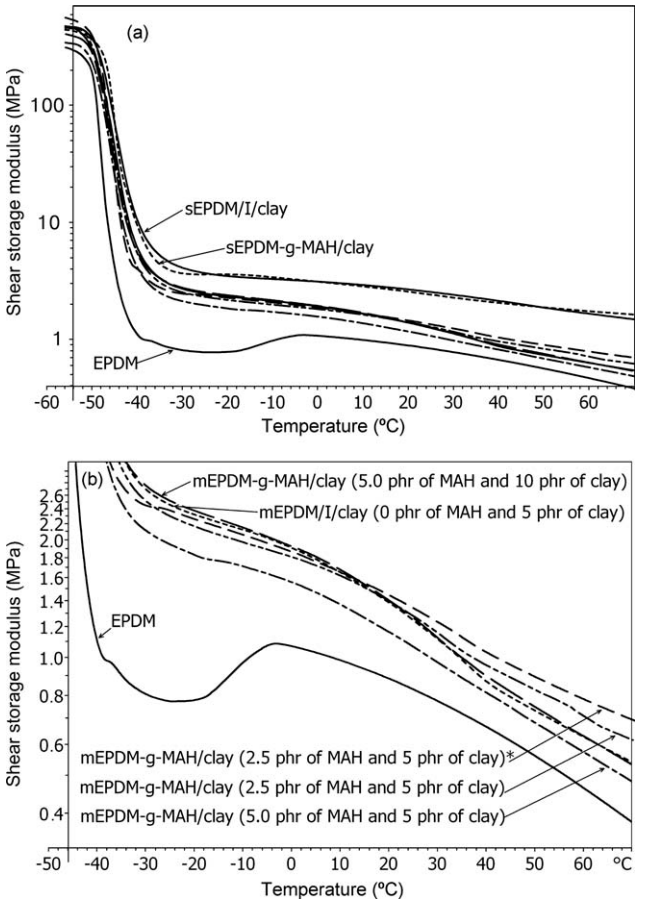

Figure 9. Shear storage modulus (G') versus temperature curves for the EPDM nanocomposites (sEPDM/I/clay, sEPDM-*g*-MAH/clay, mEPDM-*g*-MAH/clay, and mEPDM/I/clay) and for neat EPDM. (a)-curves of all samples; (b)-curves of EPDM and samples prepared by the melt method in the rubbery plateau region. *Composite was prepared by the two step method where clay was added only in the second step.

with the same clay/MAH ratio (sample with 5 phr of clay and 2.5 phr of MAH and sample with 10 phr of clay and 5.0 phr of MAH) had similar tanδ peak values.

Having in mind that the working temperature of rubbers is usually above their T_g, the plateau values of the storage modulus in this region are of great importance. Shear storage moduli (G') of the investigated composites and neat EPDM are shown in Figure 9. Note that the composites were not fully crosslinked, and thus their moduli may be compared with those of uncrosslinked rubbers. In the rubbery plateau region, G' of the uncrosslinked or not fully crosslinked polymers decreases with increasing temperature. Even though XRD analysis of sample sEPDM-*g*-MAH/clay showed that most of the clay was successfully exfoliated and that this was not the case for the sample without MAH (sEPDM/I/clay), no difference was found in the storage moduli of these two samples. However, G' values for sEPDM-*g*-MAH/clay and sEPDM/I/clay were significantly higher than that of neat EPDM. For the neat EPDM an increase of both storage and loss modulus above −20°C was observed, indicating cold crystallization. No sign of cold crystallization process was observed for any other sample. The lack of cold crystallization hints at reduced molecular mobility in the presence of clay. The composites prepared by the melt method had higher G' values than neat EPDM, but their G' values were rather low compared with those of the nanocomposites prepared via the solution method. By comparing the shear storage modulus versus temperature curve for mEPDM-*g*-MAH/clay with 5 phr of clay and 5 phr of MAH with that of mEPDM/I/clay with 5 phr of clay and no MAH, it can be seen that the G' value of the latter was higher. This is in accordance with XRD results, which showed that the use of 5 phr of MAH did not enhance the exfoliation. The sample with no MAH and 5 phr of clay had a G' curve comparable to that of the sample with 5 phr of MAH and 10 phr of clay. Among the composites prepared by the melt method, the highest moduli at room temperature and beyond were observed for composites prepared with 2.5 phr of MAH. This is again in accordance with XRD results (cf. Figure 6), which showed the best exfoliation for these samples.

CONCLUSIONS

This work was devoted to EPDM maleation and simultaneous EPDM/clay nanocomposite preparation by the solution and melt processes. The blends were reinforced with organophilic montmorillonite. EPDM maleation efficiency was investigated by FTIR-ATR spectroscopy. Clay exfoliation in the rubber matrix and the resulting nanocomposite properties were determined by XRD and DMA analyses, respectively. On the basis of the obtained results, it can be concluded that EPDM maleation and simultaneous production of EPDM/clay nanocomposites with exfoliated clay layers can be carried out in both solution and melt. For specific EPDM optimum amounts of initiator and MAH should be chosen. Too high initiator concentration causes extensive EPDM crosslinking and scission reactions during maleation. The latter are especially important for the melt process when the selected EPDM contains a high amount of polypropylene. Extensive scission of partially crosslinked EPDM chains and the shear-assisted disruption of the crosslinked network structure resulted in lower storage moduli of nanocomposites prepared by the melt process. The moduli of nanocomposites obtained in solution were higher than those produced in the melt. On the other hand, too high concentration of MAH (5 phr or more) did not improve the clay exfoliation in melt, because the shearing in the mixing chamber was significantly reduced after MAH addition. The use of relatively low MAH concentration is recommended for solution, provided that the extent of grafting is not affected. To overcome this problem, a two step melt mixing process was suggested. Accordingly, organoclay may be added to EPDM and MAH in the first or second step together with fresh EPDM.

ACKNOWLEDGMENTS

This work was performed in the framework of the following projects: Bilateral cooperation between Hungary and Slovenia (BI-HU/10-11-009). The financial support of this work by the Slovenian Ministry of Higher Education, Science and Technology (Grant P2-0191) is gratefully acknowledged. This work was also supported by the New Széchenyi Plan in Hungary (Project ID: TÁMOP-4.2.1/B-09/1/KMR-2010-0002).

REFERENCES

1. Gatos, K. G.; Karger-Kocsis, J. In Rubber Nanocomposites: Preparation, Properties and Applications; Sabu, T.; Ranimol, S., Eds.; Wiley: Singapore, **2010**; Chapter 7, p 169.
2. LeBaron, P. C.; Wang, Z.; Pinnavaia, T. J. *Appl. Clay Sci.* **1999,** *15*, 11.
3. Alexandre, M.; Dubois, P. *Mater. Sci. Eng. R: Reports* **2000,** *28*, 1.
4. Ray, S. S.; Okamoto, M. *Prog. Polym. Sci.* **2003,** *28*, 1539.
5. Karger-Kocsis, J.; Wu, C. M. *Polym. Eng. Sci.* **2004,** *44*, 1083.
6. Sengupta, R.; Chakraborty, S.; Bandyopadhyay, S.; Dasgupta, S.; Mukhopadhyay, R.; Auddy, K.; Deuri, A. S. *Polym. Eng. Sci.* **2007,** *47*, 1956.
7. Maiti, M.; Bhattacharya, M.; Bhowmick, A. K. *Rubber Chem. Technol.* **2008,** *81*, 384.
8. Wu, Y. P.; Ma, Y.; Wang, Y. Q.; Yhang, L. Q. *Macromol. Mater. Eng.* **2004,** *289*, 890.
9. Zheng, H.; Zhang, Y.; Peng, Z. L.; Zhang, Y. X. *Polym. Test.* **2004,** *23*, 217.
10. Usuki, A., Tukigase, A.; Mato, M. *Polymer* **2002,** *43*, 2185.
11. Zheng, H.; Zhang, Y.; Peng, Z. L.; Zhang, Y. X. *Polym. Polym. Compos.* **2004,** *12*, 197.
12. Ahmadi, S. J.; Huang, Y. D.; Wei, L. *Iran. Polym. J.* **2004,** *13*, 415.
13. Chang, Y. W.; Yang, Y.; Ryu, S.; Nah, C. *Polym. Int.* **2002,** *51*, 319.
14. Gatos, K. G.; Thomann, R.; Karger-Kocsis, J. *Polym. Int.* **2004,** *53*, 1191.
15. Gatos, K. G.; Apostolov, A. A.; Karger-Kocsis, J. *Mater. Sci. Forum.* **2005,** *482*, 347.
16. Gatos, K. G.; Karger-Kocsis, J. *Polymer* **2005,** *46*, 3069.
17. Acharya, H.; Pramanik, M.; Srivastava, S. K.; Bhowmick, A. K. *J. Appl. Polym. Sci.* **2004,** *93*, 2429.
18. Acharya, H.; Srivastava, S. K. *Macromol. Res.* **2006,** *14*, 132.
19. Ma, Y.; Wu, Y. P.; Wang, Y. Q.; Zhang, L. Q. *J. Appl. Polym. Sci.* **2006,** *99*, 914.
20. Mohammadpour, Y.; Katbab, A. A. *J. Appl. Polym. Sci.* **2007,** *106*, 4209.
21. Gao, G.; Zhang, Z.; Li, Q.; Meng, Q.; Zheng, Y.; Jin, Z. *J. Nanosci. Nanotechnol.* **2010,** *10*, 7031.
22. Lu, Y. L.; Ye, F. Y.; Mao, L. X.; Li, Y.; Zhang, L. Q. *Express Polym. Lett.* **2011,** *5*, 777.
23. Li, W.; Huang, Y. D.; Ahmadi, S. J. *J. Appl. Polym. Sci.* **2004,** *94*, 440.
24. Mohammadpour, Y.; Katbab, A. A. *J. Appl. Polym. Sci.* **2011,** *120*, 3133.
25. Kang, D.; Kim, D.; Yoon, S. H.; Kim, D.; Barry, C.; Mead, J. *Macromol. Mat. Eng.* **2007,** *292*, 329.
26. Manjhi, S.; Sarkhel, G. J. *Appl. Polym. Sci.* **2011,** *119*, 2268.
27. Machado, A. V.; Covas, J. A.; van Duin, M. *Polymer,* **2001,** *42*, 3649.
28. van Duin, M. *Macromol. Symp.*, **2003,** *202*, 1.
29. Heinen, W.; Rosenmöller, C. H.; Wenzel, C. B.; de Groot, H. J. M.; Lugtenburg, *J. Macromolecules* **1996,** *29*, 1151.
30. Ranganathan, S.; Baker, W. E.; Russel, K. E.; Whitney, R. A. *J. Polym. Sci. Part A: Polym. Chem.* **1999,** *37*, 3817.
31. Gaylord, N. G.; Mehta, M.; Mehta, R. *J. Appl. Polym. Sci.* **1987,** *33*, 2549.
32. Oostenbrink, A. J.; Gaymans, R. J. *Polymer* **1992,** *33*, 3086.
33. Wu, C. H.; Su, A. C. *Polym. Eng. Sci.* **1991,** *31*, 1629.
34. Grigoryeva, O. P.; Karger-Kocsis, J. *Eur. Polym. J.* **2000,** *36*, 1419.
35. De Vitto, G.; Lanzetta, N.; Maglio, G.; Malinconico, M.; Musto, P.; Palumbo, R. *J. Polym. Sci. Polym. Chem. Ed.* **1984,** *22*, 1335.
36. Cimmino, S.; D'Orazio, L.; Greco, R.; Maglio, G.; Malinconico, M.; Martuscelli, E.; Palumbo, R.; Ragoista, G. *Polym. Eng. Sci.* **1984,** *24*, 48.
37. Xie, H. Q.; Feng, D. S.; Guo, J. S. *J. Appl. Polym. Sci.* **1997,** *64*, 329.
38. Greco, R.; Maglio, G.; Musto, P. *J. Appl. Polym. Sci.* **1987,** *37*, 2513.
39. Greco, R.; Maglio, G.; Musto, P.; Scarinzi, G. *J. Appl. Polym. Sci.* **1989,** *37*, 777.
40. Greco, R.; Musto, P.; Riva, F.; Maglio, G. *J. Appl. Polym. Sci.* **1989,** *37*, 789.
41. Greco, R.; Musto, P. J. *Appl. Polym. Sci.* **1992,** *44*, 781.
42. Liu, B. L.; Ding, Q. J.; He, Q. H.; Cai, J.; Hu, B. X.; Shen, J. *J. Appl. Polym. Sci.* **2006,** *99*, 2578.
43. Ahmadi, S. J.; Huang, Y. D.; Li, W. *Compos. Sci. Technol.* **2005,** *65*, 1069.
44. Samay, G.; Nagy, T.; White, J. L. *J. Appl. Polym. Sci.* **1995,** *56*, 1423.
45. Varghese, S.; Karger-Kocsis, J.; Gatos, K. G. *Polymer,* **2003,** *44*, 3977.